AGU PUBLICATIONS

JGR

Journal of Geophysical Research: Oceans

RESEARCH ARTICLE

10.1002/2014JC009956

Key Points:
- Wave-stirring-induced mixing parameterization scheme is added to a coupled model
- Wave-stirring-induced mixing has significant impacts on SST simulation
- Wave-stirring-induced mixing impacts the initialization and integration of model

Correspondence to:
S.-Q. Peng,
speng@scsio.ac.cn

Citation:
Li, Y., S. Peng, J. Wang, and J. Yan (2014), Impacts of nonbreaking wave-stirring-induced mixing on the upper ocean thermal structure and typhoon intensity in the South China Sea, *J. Geophys. Res. Oceans*, *119*, doi:10.1002/2014JC009956.

Received 20 MAR 2014
Accepted 16 JUL 2014
Accepted article online 21 JUL 2014

Impacts of nonbreaking wave-stirring-induced mixing on the upper ocean thermal structure and typhoon intensity in the South China Sea

Yineng Li[1], Shiqiu Peng[1], Jia Wang[2], and Jing Yan[1]

[1]State Key Laboratory of Tropical Oceanography, South China Sea Institute of Oceanology, Chinese Academy of Sciences, Guangzhou, China, [2]NOAA Great Lakes Environmental Research Laboratory, Ann Arbor, Michigan, USA

Abstract To investigate the effect of nonbreaking wave-induced mixing caused by surface wave stirring on the upper ocean thermal structure (UOTS) and the typhoon intensity, a simple nonbreaking wave-stirring-induced mixing parameterization (WMP) scheme is incorporated into a regional coupled atmosphere-ocean model for the South China Sea (SCS), which couples the Princeton Ocean Model (POM) to the Weather Research and Forecasting (WRF) model using the OASIS3 coupler. The results of simulating two selected typhoon cases indicate that the nonbreaking wave-stirring-induced mixing has significant impacts on UOTS and the typhoon intensity, and the incorporation of the simple WMP scheme in the coupled model helps to improve the simulation of UOTS and thus the typhoon intensity. In the case that the typhoon intensity is underestimated by the atmosphere model alone, the improvement of initial UOTS by the ocean model with the WMP included can deepen the initial thermocline depth, reduce the effect of SST cooling, and prevent the typhoon intensity from undesired weakening. In the case that the typhoon intensity is overestimated (with strong winds), including the WMP in the ocean model significantly enhances the total vertical mixing rate in the upper ocean, which in turn enhances the SST cooling and thus reduces the typhoon intensity as desired. The results obtained in this study make a contribution to the ongoing efforts of improving the typhoon intensity forecast using a regional atmosphere-ocean coupled model by worldwide researchers and forecasters, especially for the typhoons in the SCS regions.

1. Introduction

The South China Sea (SCS) is the largest marginal sea in the tropics with a maximum depth of more than 5000 m (Figure 1). It covers an area from the equator to 23°N and from 99°E to 121°E and connects to the East China Sea to the northeast, the Pacific Ocean and the Sulu Sea to the east, and the Java Sea and the Indian Ocean to the southwest. Climatic variations in the atmosphere and in the upper ocean of the SCS are dominated by the East Asian monsoon system [*Wyrtki*, 1961; *Wu and Wang* 2002a, 2002b; *Su*, 2004]. It is an area where tropical cyclones (TCs) occur frequently in the summer and fall, causing huge property damage and life loss each year in the Philippines, Vietnam, and China [*Wu and Kuo*, 1999]. One example is typhoon Haiyan (2013), which is the deadliest Philippine typhoon on record, killing at least 6201 people in that country alone [http://en.wikipedia.org/wiki/Typhoon_Haiyan]. Therefore, the prediction of the atmospheric and oceanic environment in this region is attracting more attention from scientists around the world and also from the local governments and people in the region. However, the lack of skill in TCs intensity forecasts makes it difficult for the government to prepare for the arrival of TCs [*Evans and Falvey*, 2013]. This may be due to deficiencies in the atmospheric models, such as insufficient grid resolution, inadequate surface and boundary-layer formulations, and the lack of full coupling to a dynamic ocean model.

TC intensity is dominated by two factors: internal variability and environmental interactions. Many research projects on the influence of environmental interactions on TC intensity have focused on the interactions between TC and the atmospheric environment, including interactions with upper tropospheric troughs and the influence of environmental wind shear [e.g., *Emanuel et al*., 2004; *Hendricks et al*., 2010]. Nevertheless, another important aspect of environmental interactions is the coupling between the TC and the underlying ocean [*Ooyama*, 1969]. Presently, researchers are beginning to recognize that the upper ocean thermal structure (UOTS) and the ocean heat content contained between the sea surface and the depth of the 26°C

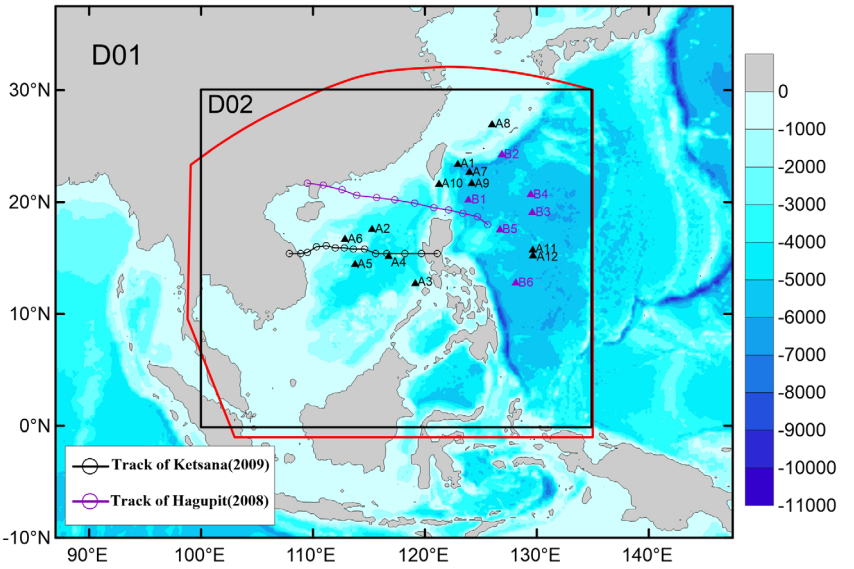

Figure 1. Configuration of the domains for each component of the ReCAM_SCS and the ocean bathymetry (unit: m). D01 and D02 represent the outer and inner domains of the atmosphere model, respectively, D02 also represent the domains of wave model, and the red frame indicates the domain of the ocean model. Also indicated in the figure are the best tracks of Ketsana (2009) and Hagupit (2008), the Argo positions A1–A12 and B1–B6 which are referred to in other figures.

isotherm (D26) may play an important role in TC intensity changes [e.g., *Shay et al*., 2000; *Ginis*, 2002]. Therefore, the coupling between the atmosphere and the ocean is important to the simulation of TC intensity, and a correct representation of the UOTS in the ocean model is a key to success of the simulation. In the SCS, however, most ocean models usually underestimate the surface mixed-layer depth during the spring-summer compared to observations, due to insufficient warming and vertical mixing [*Martin*, 1985; *Cai and Gan*, 2000]. To reduce the model bias in simulating the UOTS, one common method is to employ a data assimilation approach in the initialization of the ocean model. In practice, however, it is difficult to obtain sufficient subsurface observations along TC tracks. Moreover, the data assimilation, in which the underlying physical mechanisms are still unresolved, cannot actually improve the model physics by simply restoring the model with the "poorly-tuned" mixing processes to the measurements. Therefore, the search for a better representation of mixing processes in a coupled model for SCS is necessary and thus becomes a major purpose of this study.

Surface wave stirring is increasingly regarded as an important mechanism of the vertical fluxes in the upper layer ocean [*Babanin*, 2006]. Apart from the wave-breaking mixing which exists at depths comparable with the wave height [*Terray et al*., 1996; *Babanin et al*., 2005], the nonbreaking wave-stirring-induced vertical mixing caused by wave stirring can directly affect or influence the upper ocean mixing down to depths of the order of 100 m [*Babanin*, 2006; *Babanin and Haus*, 2009]. The wave-stirring-induced mixing is supposed to facilitate the upper ocean mixing, because it can transfer kinetic energy from surface waves to ocean circulation through the processes of vertical wave motion and the wave-induced Reynolds stress. This has been revealed in a number of laboratory experiments [e.g., *Babanin and Haus*, 2009; *Dai et al*., 2010], theoretical studies [e.g., *Ardhuin and Jenkins*, 2006; *Huang and Qiao*, 2010], and numerical investigations [e.g., *Pleskachevsky et al*., 2011; *Qiao et al*., 2004, 2008, 2010; *Gayer et al*., 2006, *Babanin et al*., 2009; *Huang et al*., 2012]. Field observations of water temperature further highlight that wave-stirring-induced mixing is important to the upper ocean during the passage of a TC [*Toffoli et al*., 2012]. Although the effect of the wave-stirring-induced mixing is found to be small at low-latitude ocean (south of 25°N) due to relatively small amplitude of the wind-generated waves [*Qiao et al*. 2008], it is significant in the SCS where the mixed-layer depth (MLD) is relatively shallow during the warm season, especially under high wind conditions (like TCs). It is thus worth investigating the impacts of wave-stirring-induced mixing on the UOTS of the SCS and the TC intensity simulation. For this purpose, this study incorporates a simplified wave-stirring-induced mixing parameterization (WMP) scheme in a regional atmosphere-ocean coupled model for the SCS (denoted as ReCAM-SCS) and performs a set of sensitivity simulation tests for real typhoon cases.

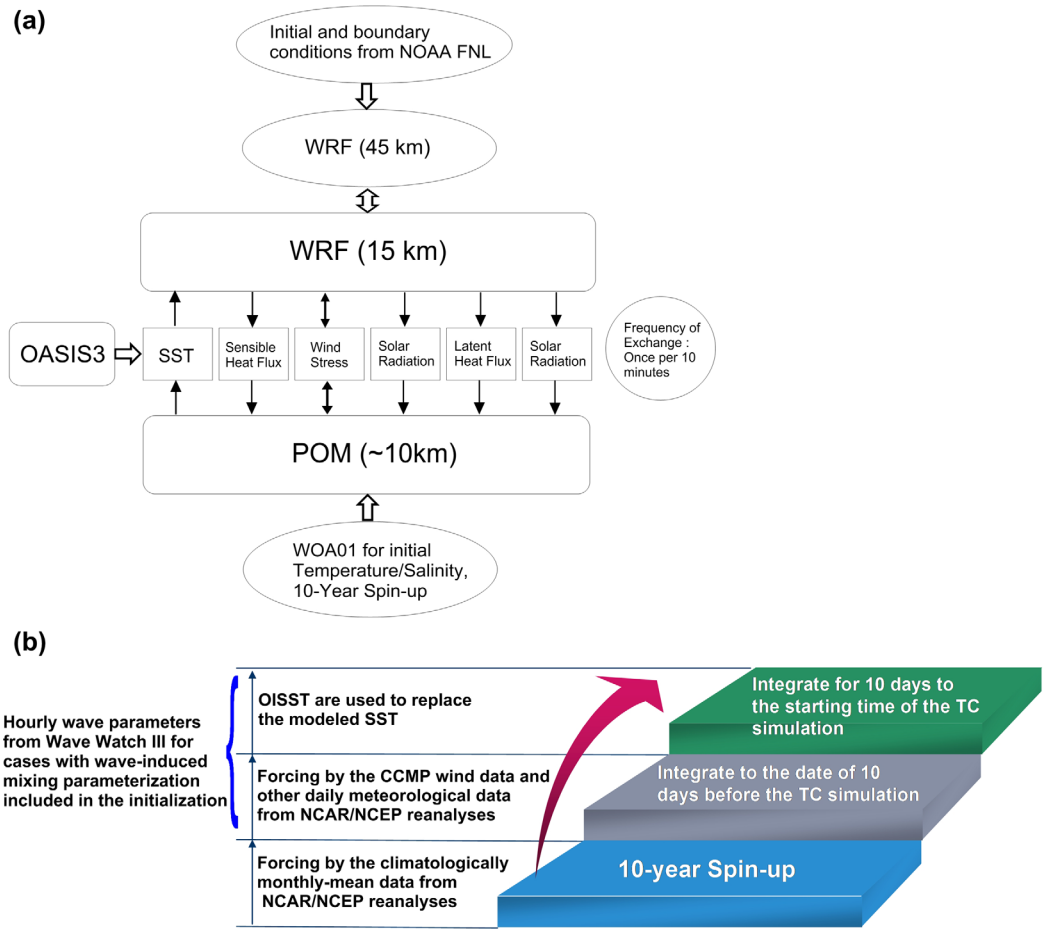

Figure 2. (a) The coupled atmosphere-ocean system and (b) the procedure of the ocean model initialization.

The next section gives a brief introduction of the developed regional air-sea coupled model ReCAM-SCS. Section 3 describes the model initialization and, wind-wave-induced mixing parameterization, as well as the simulation test design. Simulation results are presented and analyzed in section 4, followed by the conclusions in section 5.

2. Model Description

A regional atmosphere-ocean coupled model for the SCS (hereafter denoted as ReCAM-SCS) has been developed and is employed in the present study. ReCAM-SCS includes the following three components: an atmosphere model, an ocean model, and a coupler (Figure 2a). The atmosphere model employed in the ReCAM-SCS is the Weather Research and Forecasting (WRF) model with the Advanced Research WRF (ARW) core [*Skamarock et al.*, 2007]. Details about the WRF model are referred to the papers of *Skamarock et al.* [2007] and *Wang et al.* [2007]. A two-domain configuration with "two-way" nesting is designed for the atmospheric component of ReCAM-SCS, as shown in Figure 1. The outer domain (D01) of WRF model covers the western Pacific Ocean, the entire SCS, and the eastern Indian Ocean, with a horizontal resolution of 45 km. The SST for D01 is prescribed from the daily real-time, global, sea surface temperature (RTG_SST) analysis developed at the National Centers for Environmental Prediction/Marine Modeling and Analysis Branch (NCEP/MMAB) (http://polar.ncep.noaa.gov/sst). The inner domain (D02) of WRF model, which couples with the ocean model, covers the entire SCS and southern China, with a horizontal resolution of 15 km. Both domains have 30 layers in the vertical. The Ferrier microphysics scheme [*Ferrier et al.*, 2002], Kain-Fritsch cumulus scheme [*Kain and Fritsch*, 1990, 1993], Yonsei University planetary boundary layer (YSU PBL)

scheme [*Hong et al*., 2006], and Dudhia short wave [*Dudhia*, 1989] and Rapid Radiative Transfer Model (RRTM) long wave [*Mlawer et al*., 1997] radiation schemes are chosen for both domains.

The Princeton Ocean Model (POM) [*Blumberg and Mellor*, 1987] is adopted as the ocean component of ReCAM-SCS. POM is a three dimensional, fully nonlinear, primitive equation ocean model. It includes the 2.5 order turbulence closure scheme of *Mellor and Yamada* [1982] to calculate turbulence viscosity and diffusivity. The model domain (Figure 1) is from −1°N to 32°N and 99°E to 135°E, with horizontal grids refined on the SCS spacing averagely of 10 km, and 23 vertical sigma layers, 9 of which in the upper 200 m for a depth of 1000 m. A 1 arc min global relief model of Earth's topography and bathymetry (ETOPO1) [*Marks and Smith*, 2006] is used in the model. At the nearshore, the model's minimum depth is set to 10 m, based on a physical stability criterion of the global stability of *Wang* [1996]: $h_{\min}+\zeta_{\max}>0$ where $h_{\min}$ is the minimum water depth, and $\zeta_{\max}$ is the maximum water elevation possibly caused by strong (gust) winds and storm surges along the coast. The external and internal time steps are set to 6 s and 240 s, respectively. Data from the Simple Ocean Data Assimilation (SODA) reanalysis [*Carton et al*., 2000a, 2000b] are used for the open boundaries of the domain. The normal advection of different variables at the open boundaries is governed by the radiation condition [*Mellor*, 2004].

The atmosphere model is coupled to the ocean model POM through a coupler OASIS3 (Ocean Atmosphere Sea Ice Soil) developed by CERFACS (the European Centre for Research and Advanced Training in Scientific Computation) [*Valcke et al*., 2000]. Through a bilinear interpolation operating in the coupler, the temporally and spatially high resolution SST computed in the ocean model is transferred to the atmospheric module (D02 of WRF), while the wind stress, heat, moisture, and radiation fluxes computed in the atmosphere model are passed into the ocean model at a frequency of every 10 min (Figure 2a).

Recently, field and laboratory observations [e.g., *Powell et al*., 2003; *Donelan et al*., 2004; *Emanuel*, 2003; *Black et al*., 2007] have shown that the drag coefficient (C_d) approaches a steady value and even decreases with increasing wind speed under high wind conditions (~33 m/s). Thus, we employ the formulas of *Large and Yeager* [2009] to calculate the wind stress for the ocean model:

$$C_d=\begin{cases} a_1/|\mathbf{v}|+a_2+a_3|\mathbf{v}|+a_4|\mathbf{v}|^6 & |\mathbf{v}|<33\ \mathrm{ms}^{-1} \\ 0.00234 & |\mathbf{v}|>33\ \mathrm{ms}^{-1} \end{cases}, \tag{1}$$

where $\mathbf{v}=\mathbf{v_a}-\mathbf{v_o}$, in which $\mathbf{v_a}$ is the wind velocity at 10 m above the surface, and $\mathbf{v_o}$ is the velocity of ocean surface currents. The parameters are set following the suggestion of *Large and Yeager* [2009] as $a_1=0.0027\,\mathrm{ms}^{-1}$, $a_2=0.000142$, $a_3=0.0000764\,(\mathrm{ms}^{-1})^{-1}$, and $a_4=-3.14807\times10^{-13}\,(\mathrm{ms}^{-1})^{-6}$.

3. Model Initialization, Wave-Induced Mixing Parameterization, and Simulation Test Design

3.1. Model Initialization

For the atmosphere model, the output from the final (FNL) Operational Global Analysis data maintained by the NCEP with horizontal resolution of $1^\circ\times1^\circ$ is used to provide initial conditions and lateral boundary conditions for the outer domain. The FNL data are from the Global Data Assimilation System (GDAS), which continuously collects observational data from the Global Telecommunications System (GTS), and other sources, for many analyses (http://rda.ucar.edu/datasets/ds083.2/).

For the ocean model, the initialization procedure includes three steps (Figure 2b). First, POM is integrated from the "cold start" of the ocean. The initial temperature and salinity are from the World Ocean Atlas 2001 (WOA01) for January [*Boyer et al*., 2002], and the climatological monthly mean wind stress and other meteorological forcing data, including net heat fluxes and short-wave radiation fluxes, are from the National Center for Atmospheric Research (NCAR)/NCEP reanalysis [*Kalnay et al*., 1996]. After 10 model years spin-up, the model reaches a quasiequilibrium state [*Zhang and Qian*, 1999]. The second procedure is to adjust the upper ocean structure to a more realistic state before starting the TC simulation. In this procedure, POM is integrated from the first of January of the year in which the TC occurred to 10 days before the date of the TC simulation. As the gustiness of wind at synoptic time scales is essential for the wave-induced mixing parameterization, the 6 hourly Cross-Calibrated Multi-Platform (CCMP) wind data with a spatial resolution of 0.25° are used in this study. The CCMP data set combines data derived from SSM/I, AMSRE, TRMM TMI, Quikscat, and other missions using a variational analysis method (VAM) to produce a consistent

climatological record of ocean surface vector winds at 25 km resolution (http://podaac.jpl.nasa.gov/PRODUCTS/p079.html). Other daily meteorological forcing data, including air temperature, humidity, and shortwave radiation fluxes, are obtained from NCAR/NCEP reanalysis. The Optimally Interpolated Sea Surface Temperature (OISST) is nudged into the surface layer of the ocean model. The OISST data are daily-averaged with 9 km spatial resolution and are provided by the Remote Sensing System (RSS), which combine different satellite data sets including TMI, AMSR-E, WindSAT, Terra MODIS, and Aqua MODIS (http://www.ssmi.com/sst/microwave_oi _sst_browse. html). In the third procedure, the OISST data are used to replace the modeled SST, and POM is integrated for 10 days to the starting time of the TC simulation for a thermal/dynamical adjustment in the upper ocean.

3.2. Wave-Stirring-Induced Mixing Parameterization

As previously mentioned, the mixed-layer depth is usually underestimated by ocean models for the SCS. To overcome this, we add the effect of wave-stirring-induced mixing in the calculation of the mixing coefficient in POM using a simple WMP scheme. Following the previous studies of *Hu et al*. [2004] and *Hu and Wang* [2010], we define a wind wave-stirring-induced mixing coefficient as

$$K_{mw}=\frac{2v^2}{g}\delta\beta^3|\mathbf{v}|^3 e^{\frac{gz}{\beta^2|\mathbf{v}|^2}}, \tag{2}$$

where β is the wave age ($0<\beta<1$ for growing waves, and $\beta=1$ for mature waves), δ the wave steepness, $z<0$ m the water depth, $v=0.4$ the von Kármán constant, and $g=9.81$ the acceleration of gravity. The wave age β is defined as

$$\beta=\frac{c_p}{|\mathbf{v}|}=\frac{g}{\omega_p|\mathbf{v}|}=\frac{gT_p}{2\pi|\mathbf{v}|}, \tag{3}$$

where c_p is the phase velocity, $\mathbf{v}=\mathbf{v_a}-\mathbf{v_o}$, ω_p the peak frequency, and T_p the peak period.

In this study, the peak wave period and the wave steepness are obtained from an off-line run of the Wave Watch III model [*Tolman*, 2009]. The domain of Wave Watch III model is the same as region D02 of WRF, but with a resolution of 0.1°. At the second and the third stage of the ocean initialization procedure, the wave model is forced by the CCMP winds and the hourly outputs of the wave parameters (peak wave period and wave steepness) are interpolated into the ocean grid; during the simulation of the TCs, the wave model is forced by the 10 m winds from WRF run without WMP included and the obtained wave parameters are input to the ocean model every 10 min.

The heat diffusion coefficient K_{hw} is calculated by $K_{hw}=\alpha\cdot K_{mw}$, where α is an empirical constant depending on the Richardson number. In POM, α is defined as

$$\alpha=\frac{S_H}{S_M}, \tag{4}$$

where S_H and S_M are the stability functions, relating to the Richardson number [*Mellor*, 2004]. Thus, the total mixing coefficients are

$$K_m^{'}=K_m+K_{mw};\quad K_h^{'}=K_h+K_{hw}, \tag{5}$$

where K_m and K_h are calculated by the 2.5 order closure turbulence scheme of *Mellor and Yamada* [1982].

3.3. Simulation Test Design

Two typhoon cases, Ketsana (2009) and Hagupit (2008), are selected for the purpose of this study. Ketsana (2009) represents the case where intensity is overestimated by the atmosphere model alone, while Hagupit (2008) represents the case where intensity is underestimated. Typhoon Ketsana (2009) formed as a tropical storm over the western Pacific at 0000 UTC 26 September 2009, and intensified to become a strong tropical storm at 2100 UTC 26 September, and a typhoon at 0200 UTC 28 September with a minimum pressure of 960 h Pa and a maximum wind speed of 40 m s^{-1}. After crossing the Philippine Islands and entering the SCS, Ketsana (2009) swept westward and made landfall on the east coast of Vietnam at 0700 UTC 29 September 2009 (Figure 1). Typhoon Hagupit (2008) formed on 14 September 2008 in the western Pacific and moved westward toward the Philippines (Figure 1). It entered the SCS on 21 September 2008 and

Table 1. Simulation Test Design

Tests	IC With WMP	Forecast With WMP
NON_WMP	No	No
INI_WMP	Yes	No
SIM_WMP	No	Yes
ALL_WMP	Yes	Yes

intensified when moving northwest to China. Finally, it made landfall near Maoming in the Guangdong Province of China at 6:45 A.M. (local time), 24 September 2008.

Four simulation tests were designed for each TC case, as shown in Table 1. NON_WMP refers to the two-way coupled test in which the WRF is coupled

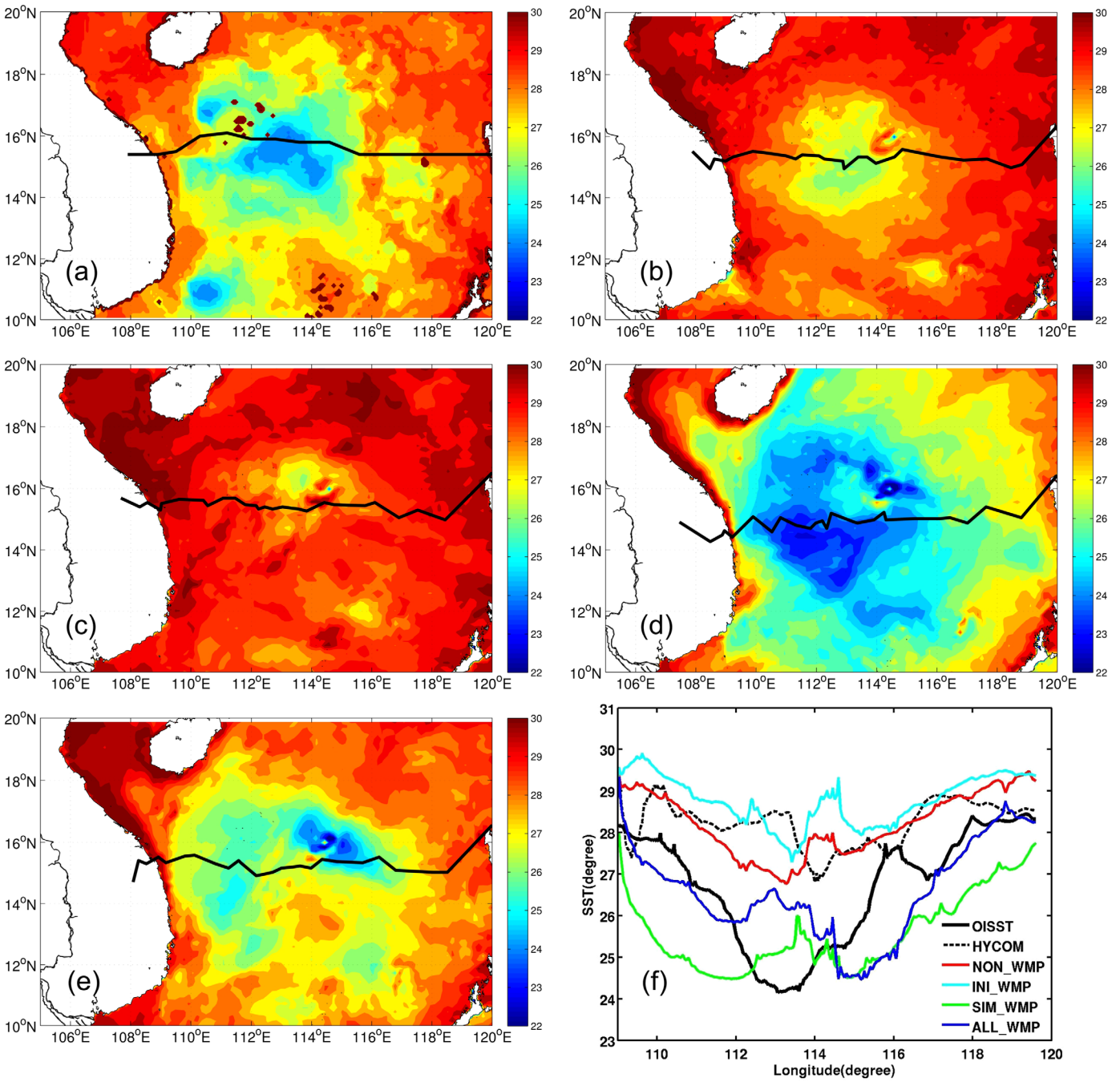

Figure 3. The spatial distributions of daily-mean SST (unit: °C) on 28 September 2009 from (a) OISST, (b) NON_WMP, (c) INI_WMP, (d) SIM_WMP, (e) ALL_WMP, as well as (f) the along-track SST (unit: °C) from observations (OISST), HYCOM reanalysism and different simulation tests for the typhoon Ketsana (2009) case. The best or simulated track is imposed on the spatial distributions of daily-mean SST (Figures 3a–3e).

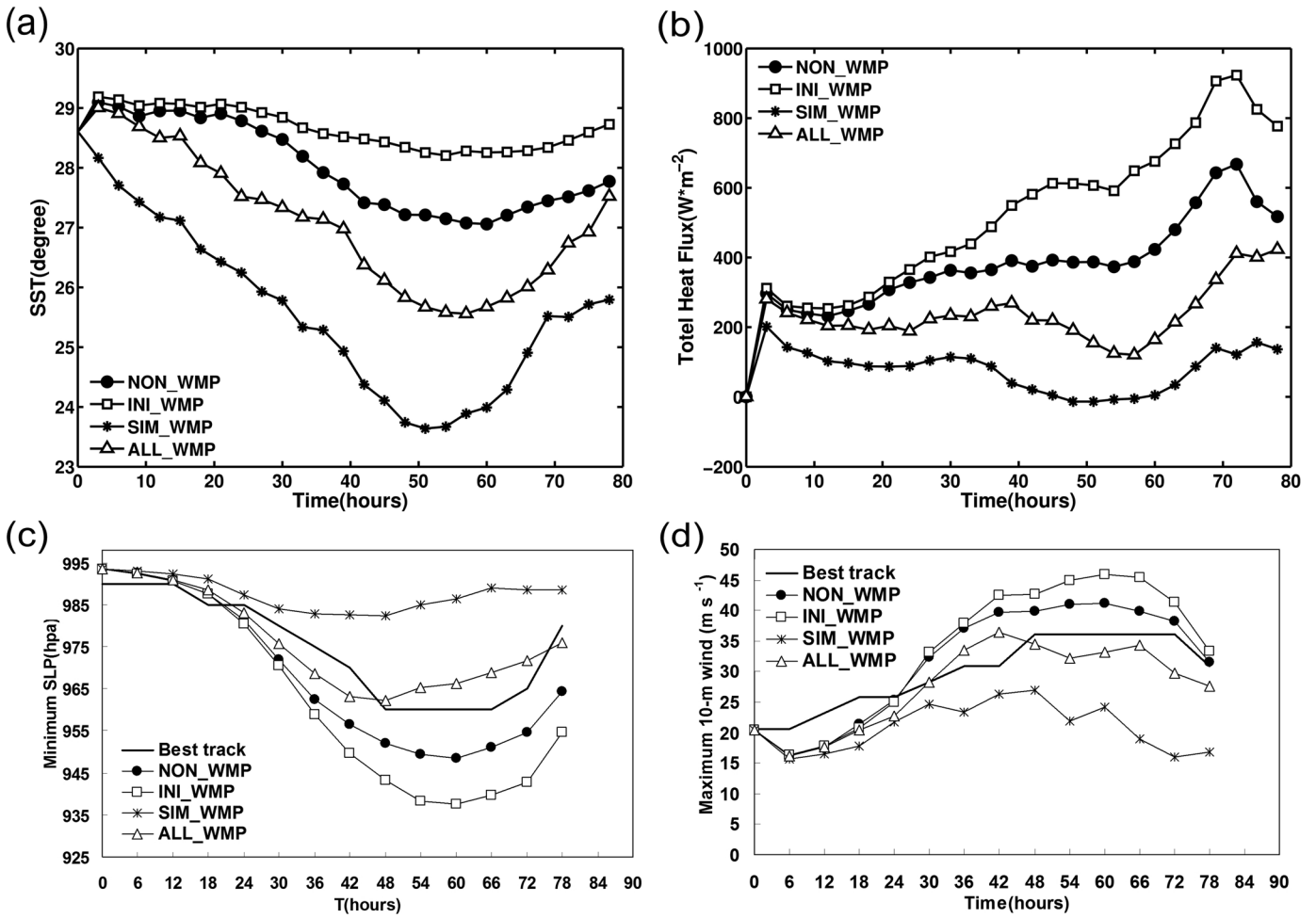

Figure 4. The temporal evolution of (a) the area-averaged SST (unit: °C) and (b) the total heat flux (unit: W m^{-2}) in the 200 km-radius inner core region, (c) the minimum sea level pressure (SLP, unit: h Pa), and (d) the maximum 10 m wind (unit: m s^{-1}) from all simulation tests and best track reanalysis data from Japan Meteorological Agency (JMA) for the typhoon Ketsana (2009) case.

to a "standard" three-dimensional ocean model POM in which the contribution of wave breaking is considered using the method of *Mellor and Blumberg* [2004]. To stand out the effect of including WMP in the ocean model on the UOTS simulations, the contribution of Langmuir Circulations to the upper ocean mixing is not included in this study. INI_WMP, SIM_WMP, and ALL_WMP are similar to NON_WMP, except that the WMP scheme is included in the initialization of the ocean model (for INI_WMP) or the TC simulation (for SIM_WMP) or both (for ALL_WMP).

For the Ketsana (2009) case, the simulation starts at 0600 UTC 26 September 2009. For the Hagupit (2008) case, the starting time of the model simulation is at 1200 UTC 21 September 2008.

4. Results and Discussion

Previous studies have indicated that SST cooling induced by strong winds has a significant impact on TC intensity, but little on TC tracks [*Marks and Shay*, *1998*; *Shay et al*., 2000;]. Similarly, the results from different simulation tests in this study indicate that incorporating the WMP in the coupled model has significant impact on SST simulation which in turn affects the TC intensity simulation but has minor effect on the TC track simulation (figure omitted). As discussed by *Marks and Shay* [1998], it is the large-scale processes that determine the TC track forecasts, whereas the mesoscale processes associated with the local air-sea

Table 2. Minimum SLP and Maximum 10 m Wind From JMA Best Track and Each Simulation Test

Typhoon Cases	Min SLP (h Pa)/Max 10 m Wind (m s^{-1})	JMA Best Track	NON_WMP	INI_WMP	SIM_WMP	ALL_WMP
Typhoon Ketsana (2009)	Min SLP (h Pa)	956	948.6	938.0	982.3	962.1
	Averaged Min SLP error (h Pa)		7.97	15.04	12.58	4.51
	Max 10 m wind (m s^{-1})	36.04	41.9	46.01	26.92	37.97
Typhoon Hagupit (2008)	Min SLP (h Pa)	935	964.1	960.7	979.8	969.6
	Averaged Min SLP error (h Pa)		29.03	27.66	34.96	30.7
	Max 10 m wind (m s^{-1})	56.6	35.3	38.9	27.0	32.7

interaction mainly influence the TC intensity. The key factors determining the rate of SST decrease in response to the strong TC wind forcing include (1) the initial upper ocean stratification or UOTS, (2) the TC moving speed, and (3) the mixing rate in the upper ocean and the variation of UOTS due to the change of the maximum surface winds. The incorporation of WMP in the ReCAM_SCS improves the SST simulation and thus affects TC intensity simulation/forecasting mainly through affecting the initial UOTS and the mixing rate in the upper ocean, which is discussed in detail in the following sections.

For the comparison of TC track and intensity, the Japan Meteorological Agency (JMA) best track reanalysis data is used as the benchmark in this paper. The JMA best track data were carried out with further review of Dvorak analysis considering the TC life stages overall and with all available data, including meteorological data such as those from surface observations (SYNOP, SHIP, and BUOY), satellite products of geostationary and polar-orbiting satellites (including scatterometer-derived wind data), and NWP (numerical weather prediction) outputs (see details from http://www.jma.go.jp). For the temperature verification, the Argo data collected during the TC passage and the daily reanalysis data from the 1/12° global HYbrid Coordinate Ocean Model (HYCOM) were used to verify the effect of WMP on UOTS in the follow sections. The Argo profiles are collected from the products in the USGODAE (US Global Ocean Data Assimilation Experiment, http://www.usgodae.org) in the area of [105°E–130°E; 10°N–30°N]. The HYCOM reanalysis data, which were produced by HYCOM nowcast with data assimilation at eddy-resolving resolution, have also been used as the initial conditions for HWRF (Hurricane Weather Research and Forecast) system and proved to be helpful for the TCs prediction [*Kim et al*., *2014*].

4.1. Results of Ketsana (2009)

The observed and simulated daily-mean SST distributions on 28 September are shown in Figure 3. It can be seen clearly that, while all simulation tests can reproduce the SST cooling along the TC track with a maximum near 113°E, the maximum magnitudes of the SST cooling from ALL_WMP/SIM_WMP are closer to the observations (about 5°C), and those from NON_WMP/INI_WMP are much smaller. The large discrepancy of SST cooling between NON_WMP and OISST implies that the surface and subsurface mixing rates are underestimated by the ocean model under the high wind condition, probably due to the lack or deficit of upper ocean physical processes such as the nonbreaking wave-stirring-induced mixing in the model. Compared to NON_WMP, the SST cooling along the TC track is intensified by both SIM_WMP and ALL_WMP, while it is weakened by INI_WMP. It should be noted that though the simulated SST of ALL_WMP preforms the best among all the tests, there are still some mismatches between modeled SST and OISST. The reasons for the mismatches could be but not limited to (1) there are still errors in the simulated TC tracks and wind fields (see Figures 3 and 4d) due to the deficiencies (such as the imperfect physical parameterization) in the atmospheric models or insufficient model resolution and (2) the effect of Langmuir Circulation is not included in our models. Figures 4a and 4b further display the temporal evolution of the SST and heat flux within a 200 km-radius inner core of the typhoon. Compared to the control test (NON_WMP), the incorporation of the WMP only in the initialization (INI_WMP) significantly weakens the SST cooling and leads to an increase of the heat flux, while the incorporation of the WMP only in the TC simulation (SIM_WMP) greatly intensifies the cooling and leads to a great reduction of the heat flux. When the WMP is included in both initialization and simulation (ALL_WMP), the simulated SST cooling (heat flux) is greatly intensified (reduced) compared to that from NON_WMP but slightly weakened (increased) compared to that from SIM_WMP, probably due to a better initial state of the UOTS produced by including the WMP in the initialization. These changes of SST cooling and heat flux due to the WMP incorporation should have impacts on the evolution of the TC intensity. Figures 4c and 4d show the temporal evolution of minimum sea level pressure (SLP) and

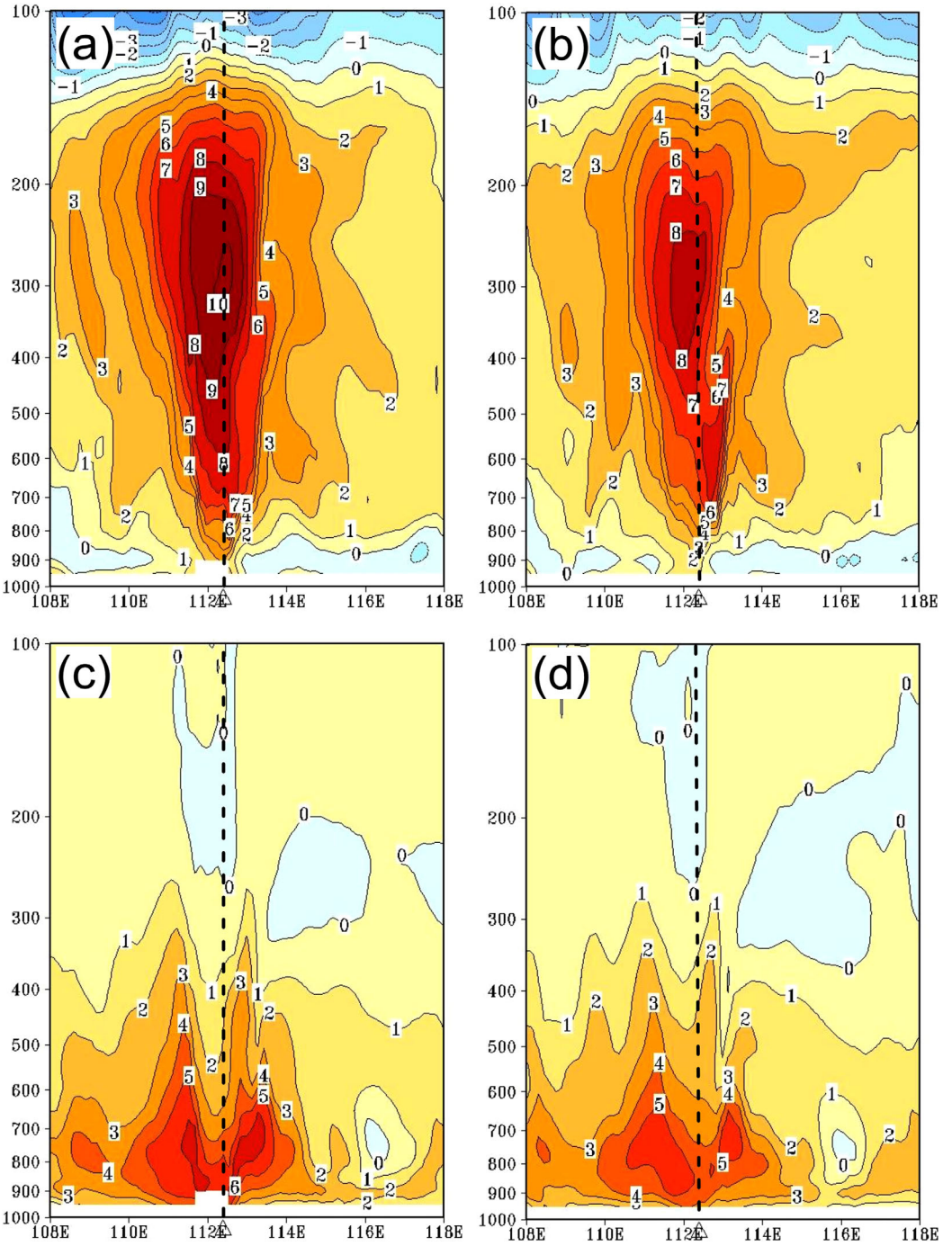

Figure 5. The height (unit: h Pa)-longitude cross sections for the anomalies of (top) the air temperature (unit: K) and (bottom) the water vapor mixing ratio (unit: kg kg^{-1}) at 0600 UTC 28 September 2009 (48 h simulation) from (a, c) NON_WMP and (b, d) ALL_WMP for the typhoon Ketsana (2009) case. The blue line denotes the TC location.

maximum 10 m wind speed from different simulation tests and the JMA best track reanalysis data. Compared to the best track reanalysis data, the NON_WMP test overestimates the TC intensity (in terms of minimum SLP) with a maximum discrepancy of 17.4 h Pa in minimum SLP (Figure 4c). This overestimated bias becomes even larger in INI_WMP up to 27.2 h Pa. SIM_WMP, however, underestimates the intensity with a maximum bias of 28.9 h Pa. These simulated intensity biases are mostly corrected in ALL_WMP, with the simulated maximum intensity closest to the observed one. The averaged minimum SLP error reduces from 7.97 h Pa for the NON_WMP to 4.51 h Pa for the ALL_WMP, or an improvement of 43.4% by the ALL_WMP

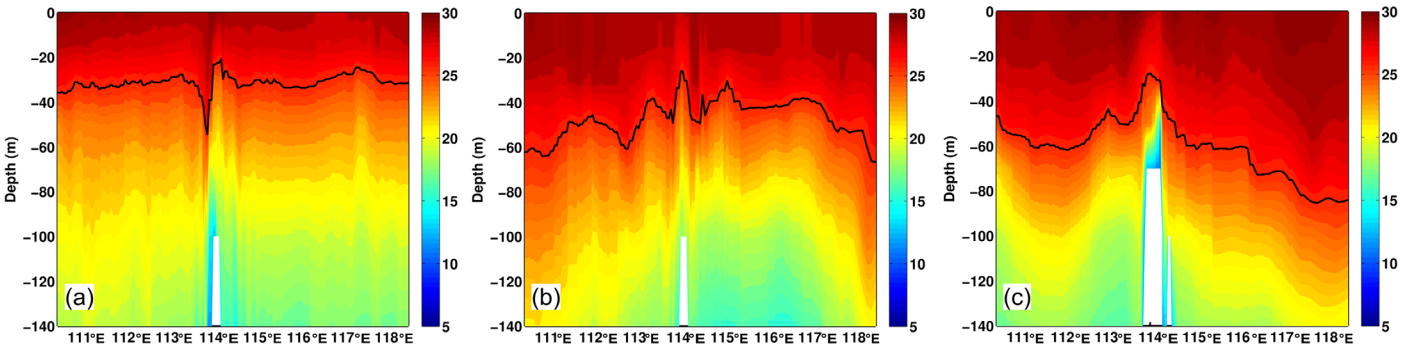

Figure 6. The depth-longitude cross sections along the best track (indicated in Figure 1) of the simulated initial sea temperature on 26 September from (a) NON_WMP/SIM_WMP, (b) INI_WMP/ALL_WMP, and (c) HYCOM reanalysis for the typhoon Ketsana (2009) case (unit: °C, the black line indicates the 26°C isotherm).

(Table 2). As to the simulated maximum wind speed (MWS), the situation is somewhat different (Figure 4d). The MWS from NON_WMP is overestimated with a mean of 41.9 m/s while that from ALL_WMP is closest to the best track reanalysis with a mean of 37.97 m/s (Table 2). INI_WMP (SIM_WMP), however, greatly overestimates (underestimates) MWS. The net weakening of the TC intensity by the incorporation of the WMP in both model initializations and runs can be seen in the water vapor mixing and air temperature in the low-middle atmosphere (Figure 5). Compared to NON_WMP (Figures 5a and 5c), both the anomalous temperature and the water vapor mixing in the inner core of the typhoon are reduced in ALL_WMP (Figures 5b and 5d), which can be attributed to the intensified SST cooling and the reduced heat flux by including the WMP in the coupled model (Figures 4a and 4b).

The above results indicate that the effect of including WMP in the initialization (INI_WMP) on the SST cooling (thus on the TC intensity) is opposite to that in the TC simulation (SIM_WMP). The reason is that including WMP in the initialization produces a well-mixed warmer upper ocean state with more heat content which suppress the SST cooling, while including WMP in the TC simulation enhances the mixing rate in the upper ocean which entrains more cold water into the surface mixed layer and thus intensifies the SST cooling, as indicated in Figures 6–8. Large differences are found in the initial subsurface sea temperature and heat content simulated by different simulation tests (Figure 6). Here we employ the depth of 26°C (D26) to represent the mixed layer of the upper ocean. Compared with a D26 of about 60–80 m in the HYCOM reanalysis, the test without the WMP included in the initialization (NON_WMP/SIM_WMP) seriously underestimates the initial MLD with a D26 $<$ 40 m. When including the WMP in the initialization (INI_WMP/

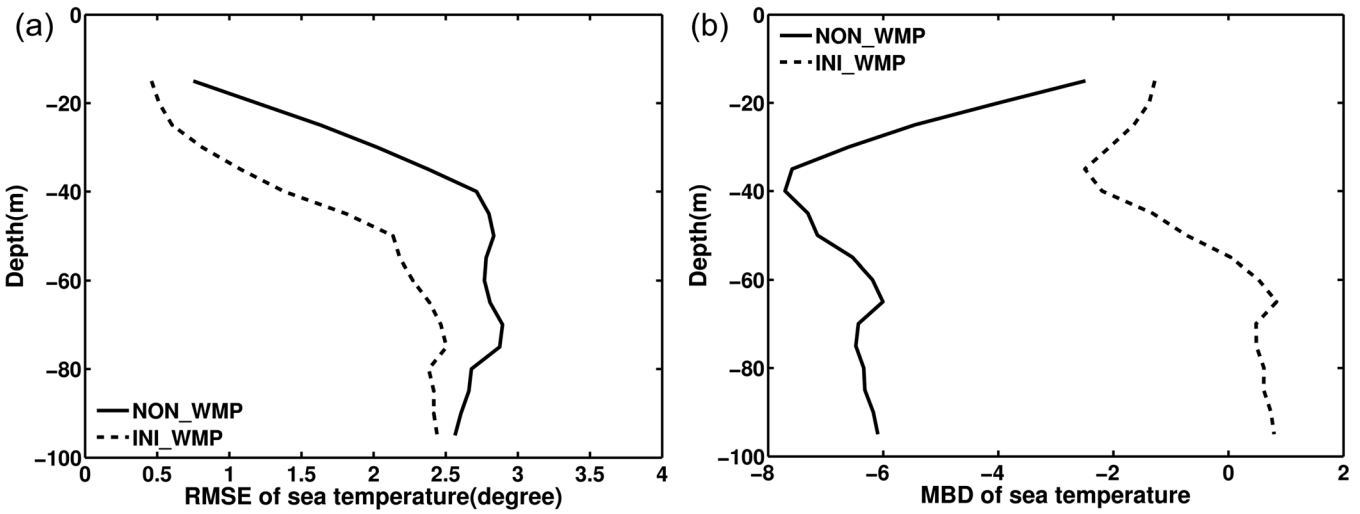

Figure 7. (a) The root-mean-square errors (RMSE, unit: °C) and (b) the mean bias deviation (MBD, unit: %) of the modeled temperature profiles against the Argos observations at locations A1–A12 (indicated in Figure 1) on 26 September 2009 for the typhoon Ketsana (2009) case (the results shown are significant with 95% confidence level).

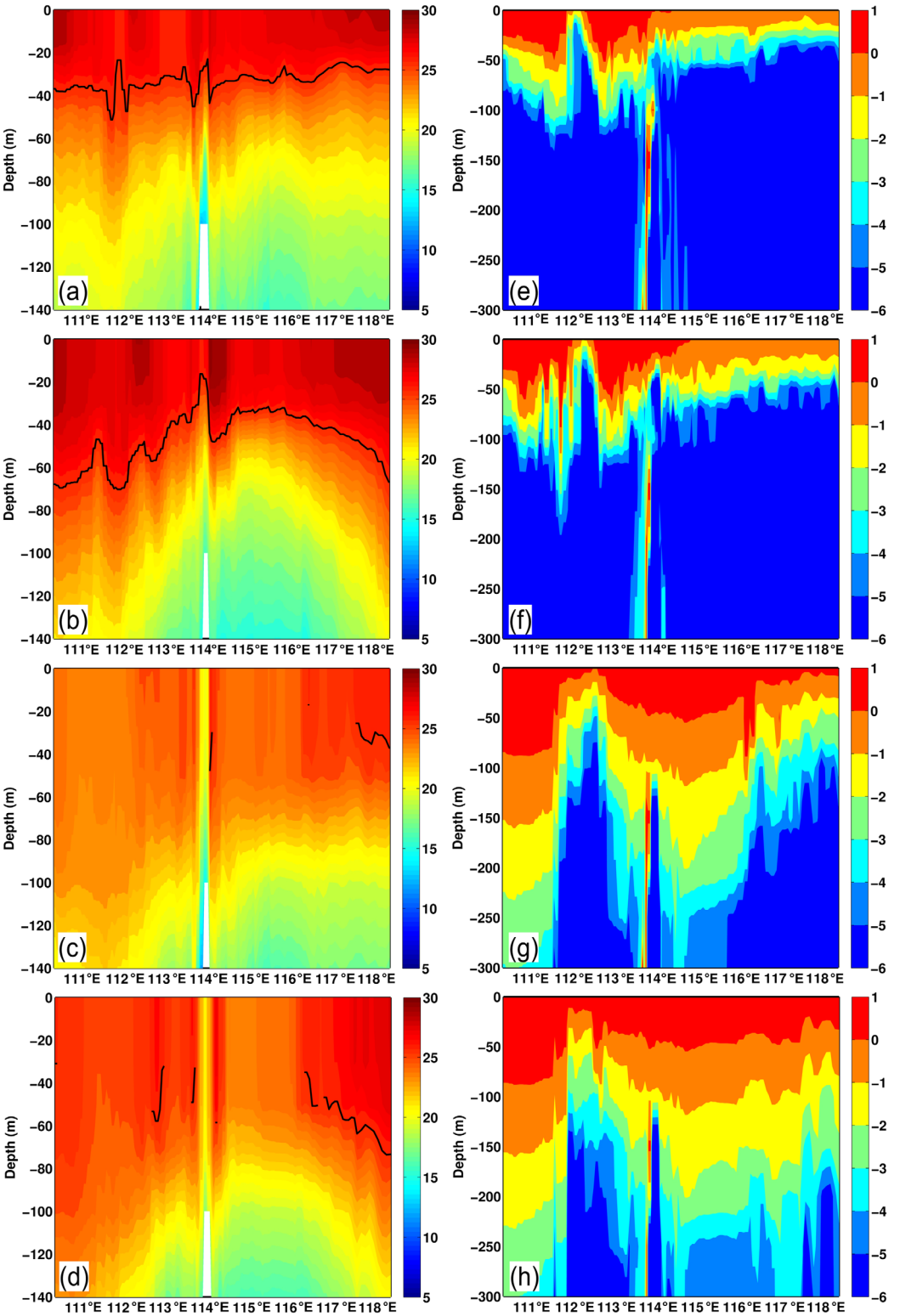

Figure 8. The depth-longitude cross sections of (left, a–d) the simulated sea temperature (unit: °C) and (right, e–h) the logarithm of vertical diffusivity at 0600 UTC 28 September 2009 (48 h simulation) along the best track (indicated in Figure 1) from (Figures 8a and 8e) NON_WMP, (Figures 8b and 8f) INI_WMP, (Figures 8c and 8g) SIM_WMP, and (Figures 8d and 8h) ALL_WMP for the typhoon Ketsana (2009) case (the black line indicates the 26°C isotherm).

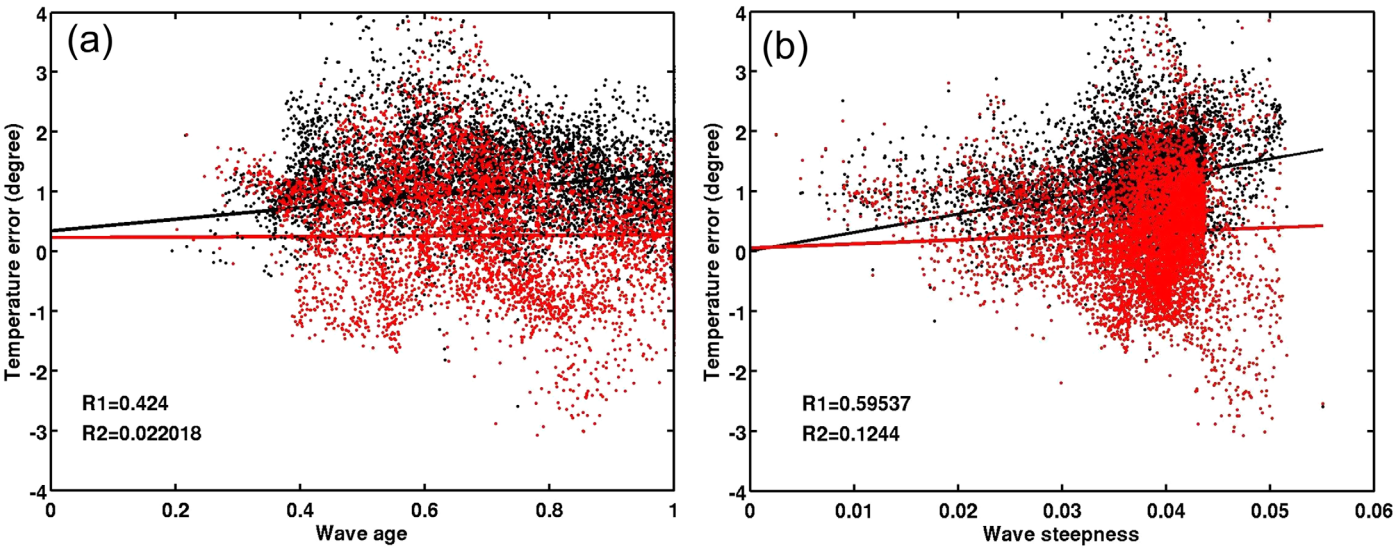

Figure 9. Scatter diagram for SST biases versus (a) wave age and (b) wave steepness for the typhoon Ketsana (2009) case. The SST biases are obtained from NON_WMP (black dots) and ALL_WMP (red dots) against OISST. R1 (R2) denotes the correlation coefficients between SST biases from NON_WM (ALL_WMP) and the wave parameters. Solid lines indicate the linear fittings of the scattering points.

ALL_WMP), however, the initial MLD is deepened with the D26 up to 60 m, which is closer to the HYCOM reanalysis. The improvements of the UOTS by including WMP in the ocean model can be more clearly seen in Figure 7, which shows the root-mean-square error (RMSE) and the mean bias deviation (MBD) of modeled sea temperature against the Argo profiles at locations A1–A12 (indicated in Figure 1). The RMSE and MBD are calculated as follows:

$$\mathrm{RMSE}=\sqrt{\frac{1}{N}\sum_{i=1}^{N}(x_i-y_i)^2}, \tag{6}$$

$$\mathrm{MBD}=100\frac{\frac{1}{N}\sum_{i=1}^{N}(x_i-y_i)}{\frac{1}{N}\sum_{i=1}^{N}y_i}=100\frac{\overline{x}-\overline{y}}{\overline{y}}\%, \tag{7}$$

where x_i and $y_i (i=1,2,3\ldots N)$ are the modeled and observed samples of any variable such as sea temperature. N is the total sampling number, and the over bars denote the average of the samples. For the tests without the WMP included in the initialization (NON_WMP/SIM_WMP), large RMSE and MBD are seen in the upper 100 m of the ocean with their maximum values up to 2.8°C and −8% near 40 m beneath the surface, respectively, indicating the initial subsurface temperature is greatly underestimated; when the WMP is included in the initialization of the model (INI_WMP/ALL_WMP), RMSE and MBD are reduced significantly in the depth from 20 m to 100 m, suggesting that the UOTS at the initial time is well reproduced with higher subsurface temperature and a deepened MLD. The thicker mixed layer contains more heat and suppresses SST cooling in the TC simulation (i.e., a negative effect), as shown in Figure 8b. On the other hand, including the WMP in the TC simulation (SIM_WMP/ALL_WMP) greatly enhances the upper ocean mixing (Figures 8g and 8h) and thus raises more cool water from under the thermocline to the surface, leading to an enhanced SST cooling (i.e., a positive effect). The reason why the mixing rate for ALL_WMP is stronger than that for SIM_WMP is that ALL_WMP simulates stronger winds (as shown in Figure 4d) due to a warmer initial sea surface produced by including the WMP in its initialization, and the nonbreaking wave-stirring-induced mixing rate is proportional to the cube of wind speed (equation (2)). The SST cooling in ALL_WMP is a compromise of the negative effect and the positive effect. In the case of TC where intensity is overestimated by the atmosphere model alone, the simulated winds are generally stronger than or comparable to the

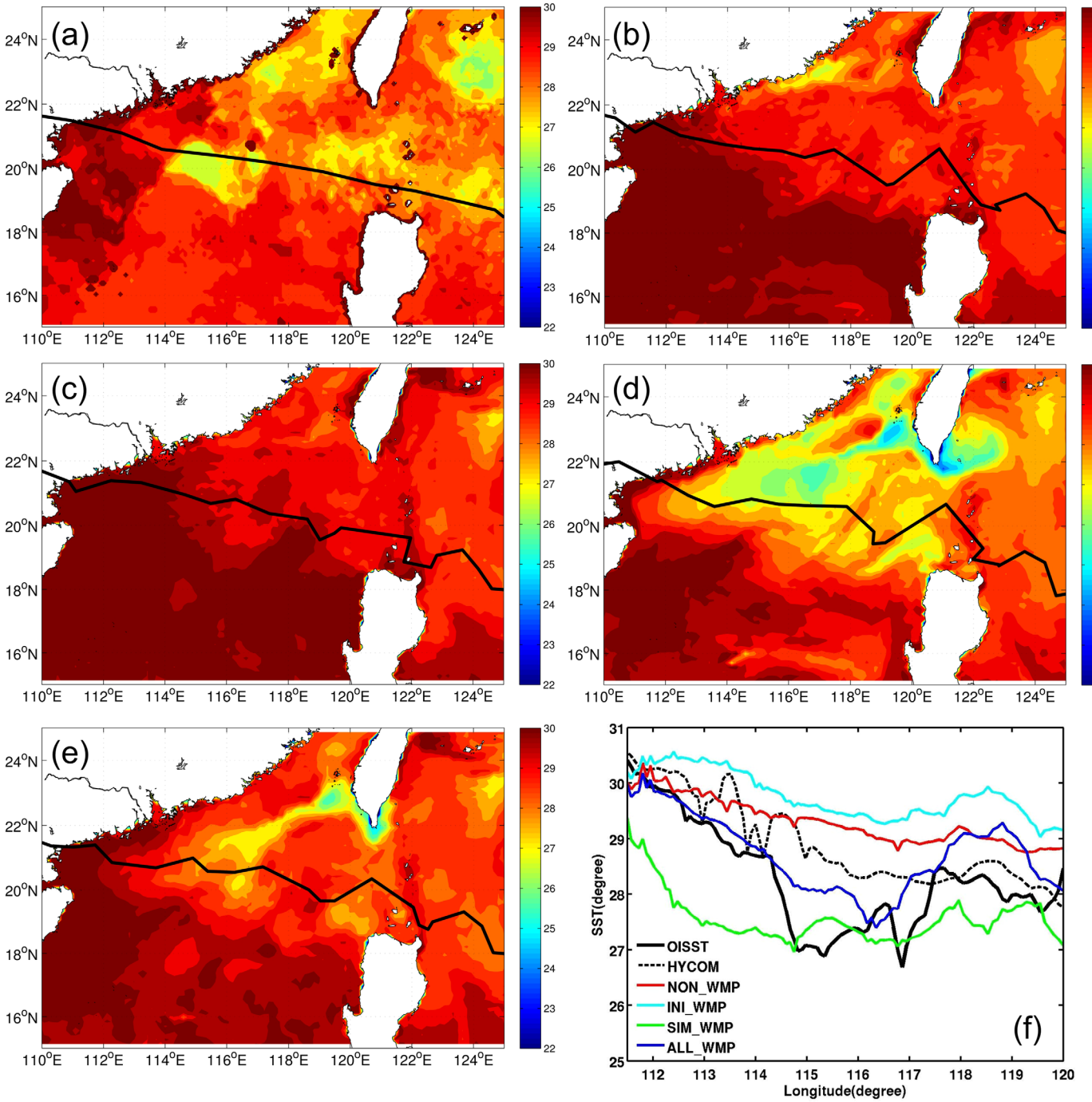

Figure 10. The spatial distributions of daily-mean SST (unit: °C) on 23 September 2008 from (a) OISST, (b) NON_WMP, (c) INI_WMP, (d) SIM_WMP, (e) ALL_WMP, as well as (f) the along-track SST (unit: °C) from observations (OISST), HYCOM reanalysis and different simulation tests for the typhoon Hagupit (2008) case. The best or simulated track is imposed on the spatial distributions of daily-mean SST (Figures 10a–10e).

observations. Therefore, the intensified upper ocean mixing plays a dominating role (positive effect) in the SST cooling over that of a deepened initial MLD by the WMP included in the initialization (negative effect). The enhanced SST cooling in turn raises the SLP and reduces the surface wind speed and heat flux, leading to a weakening of the TC intensity that is closer to the observations (Figures 4c and 4d). Therefore, for an intensity-overestimated TC, including the effect of wave-induced mixing (here with a simplified WMP) in

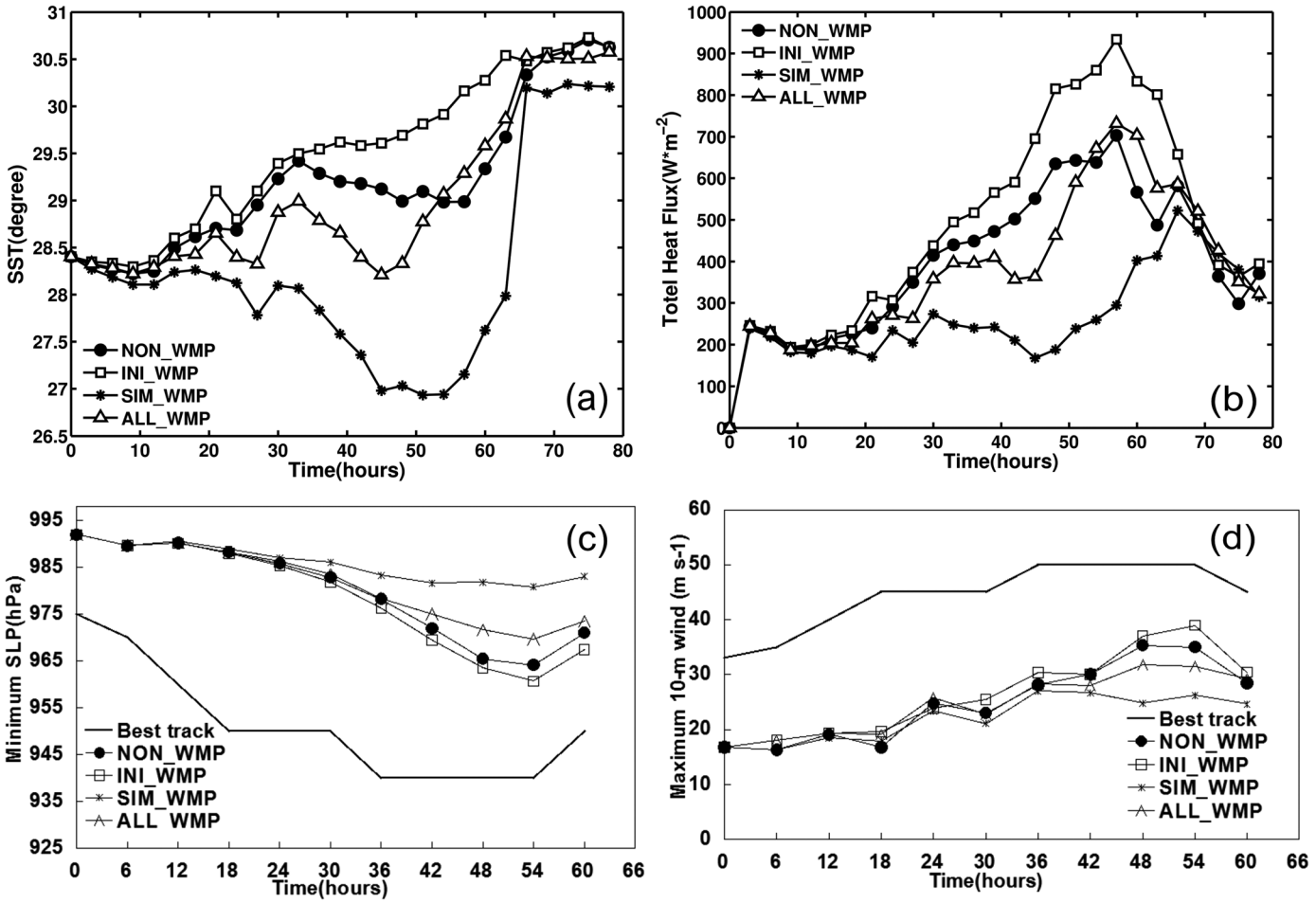

Figure 11. The time series of (a) the area-averaged SST (unit: °C) and (b) the total heat flux (unit: W m^{-2}) in the 200 km-radius inner core region from all simulation tests; (c) the minimum sea level pressure (SLP, unit: h Pa), and (d) the maximum 10 m wind (unit: m s^{-1}) from JMA and all simulation tests for the typhoon Hagupit (2008) case.

the coupled model for both the initialization and the simulation can reproduce well the UOTS and the upper ocean mixing process, leading to a better simulation of the TC intensity.

The effect of the nonbreaking wave-stirring-induced mixing on the SST can be further seen in the scatter plot of SST simulation biases versus wave age (or steepness) (Figure 9). As shown in Figure 9, the slope of a linear fitting between the SST biases and wave age (or steepness) for ALL_WMP is significantly reduced

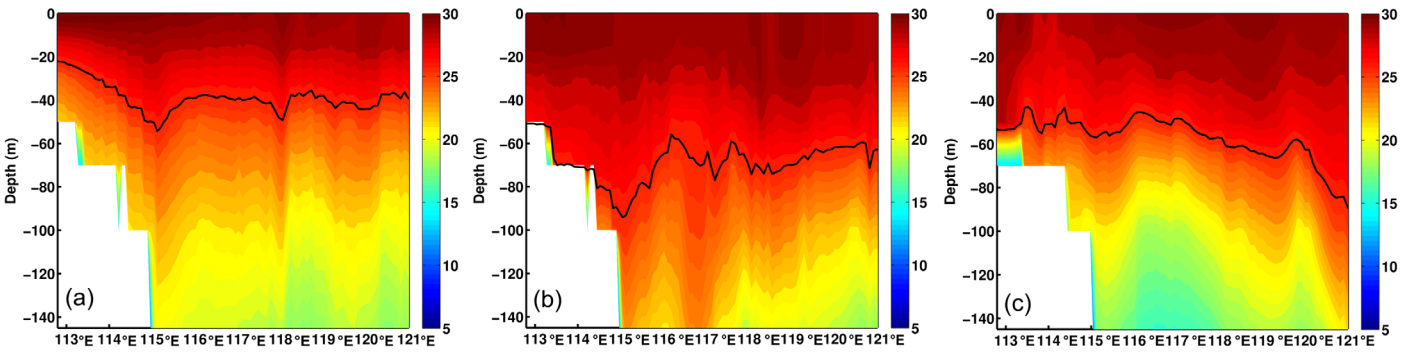

Figure 12. The depth-longitude cross sections along the best track (indicated in Figure 1) of the simulated initial sea temperature on 21 September from (a) NON_WMP, (b) INI_WMP/ALL_WMP, and (c) HYCOM reanalysis for the typhoon Hagupit (2008) case (unit: °C, the black line indicates the 26°C isotherm).

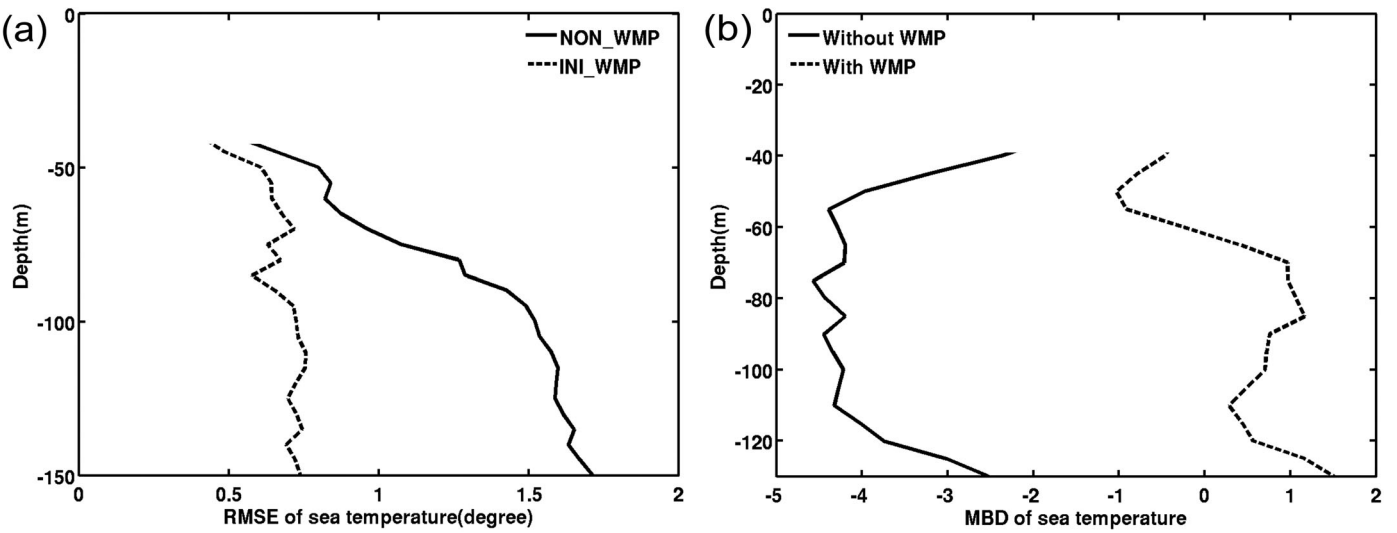

Figure 13. (a) The RMSE (unit: °C) and (b) MBD (unit: %) of the modeled temperature profiles against the Argos observations at location B1–B6 (indicated in Figure 1) for the typhoon Hagupit (2008) case (the results shown are significant with 95% confidence level).

compared to that for NON_WMP (with the correlation coefficients between SST biases and wave age/steepness reducing from 0.42/0.59 to 0.02/0.12). These results indicate that the nonbreaking wave-stirring-induced mixing indeed has significant impact on the SST and including WMP in the ocean model is able to reduce the SST biases effectively.

4.2. Results of Hagupit (2008)

The above results indicate that the incorporation of the WMP in the coupled model can intensify the SST cooling and thus weaken the TC intensity, which is desired for the intensity-overestimated TC. In the real-time forecasts of TCs, however, the opposite situation may occur, i.e., a TC may be underestimated by an atmosphere model alone. Therefore, we are most concerned about whether the TC intensity is further weakened by the incorporation of the WMP when it is already underestimated by the atmosphere model alone, which is undesired. We thus perform a set of simulation tests for the intensity-underestimated typhoon Hagupit (2008) similar to that for the intensity-overestimated typhoon Ketsana (2009). The SST cooling simulated by different tests on 23 September 2008 is shown in Figures 10 and 11a. Similar to that of Ketsana (2009), INI_WMP (SIM_WMP) weakens (intensifies) the SST cooling along the TC track with an increase (reduction) of heat flux from the ocean to the atmosphere (Figure 11b), leading to a slight intensification (weakening) in the TC intensity compared to that from NON_WMP (Figures 11c and 11d). The strength of SST cooling simulated by ALL_WMP is intermediate between INI_WMP and SIM_WMP, and the TC intensity simulated by ALL_WMP is close to that by NON_WMP with a mean error increase of 1.04 h Pa (or 3.6% of the mean error for NON_WMP) in minimum SLP and 2.6 m s^{-1} in maximum 10 m winds (Table 2). This means that the TC intensity is not significantly further weakened by the incorporation of the WMP in both the initialization and the simulation for the underestimated case. Among all simulation tests, INI_WMP performs the best whereas SIM_WMP performs the worst in the TC intensity simulation. Therefore, it is apparent that INI_WMP/ALL_WMP benefits from the initialization with the WMP included that reproduces a more realistic UOTS at the initial time, as indicated in Figures 12–14. Compared to the HYCOM reanalysis data, the initial mixing layer simulated by the ocean model without WMP included is too thin, with an offshore D26 of ~40 m offshore, while that simulated by the one with WMP included is much closer to the reanalysis data with an offshore D26 of ~70 m (Figure 12).

The deepened MLD by INI_WMP/ALL_WMP can be further verified by calculating the RMSE and MBD of the vertical distribution of the sea temperature from different simulation tests against the Argo profiles at locations B1–B6 (Figure 13). The modeled sea temperature without the WMP included in the initialization (NON_WMP/SIM_WMP) is largely underestimated between 40 and 150 m, resulting in a thin mixing layer. When the WMP is included in the initialization of the ocean model, however, the mixing layer becomes

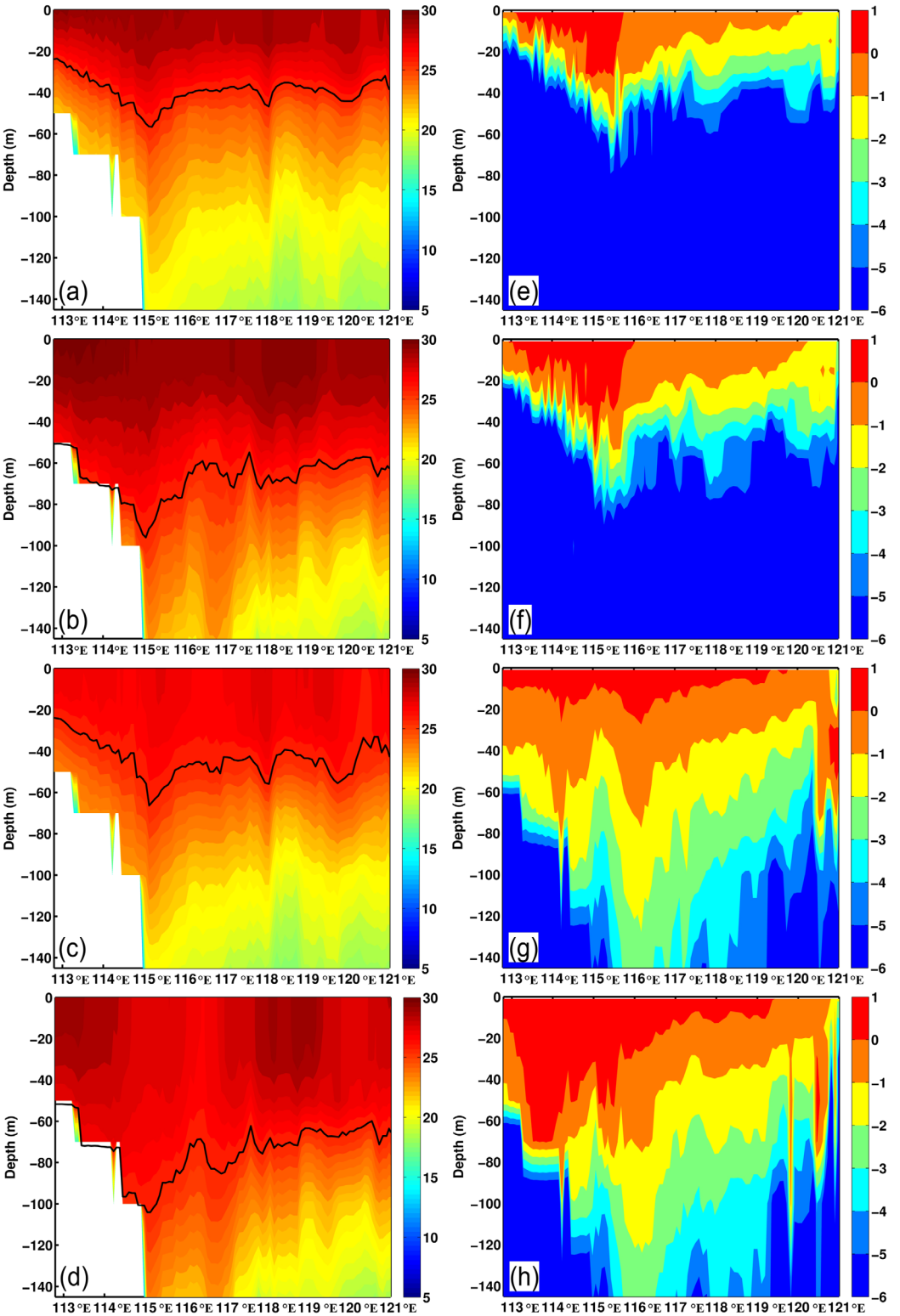

Figure 14. The depth-longitude cross sections of (left, a–d) the simulated sea temperature (unit: °C) and (right, e–h) the logarithm of vertical diffusivity at 1200 UTC 23 September 2008 (48 h simulation) along the best track (indicated in Figure 1) from (Figures 14a and 14e) NON_WMP, (Figures 14b and 14f) INI_WMP, (Figures 14c and 14g) SIM_WMP, and (Figures 14d and 14h) ALL_WMP for the typhoon Haguipit (2008) case (the black line indicates the 26°C isotherm).

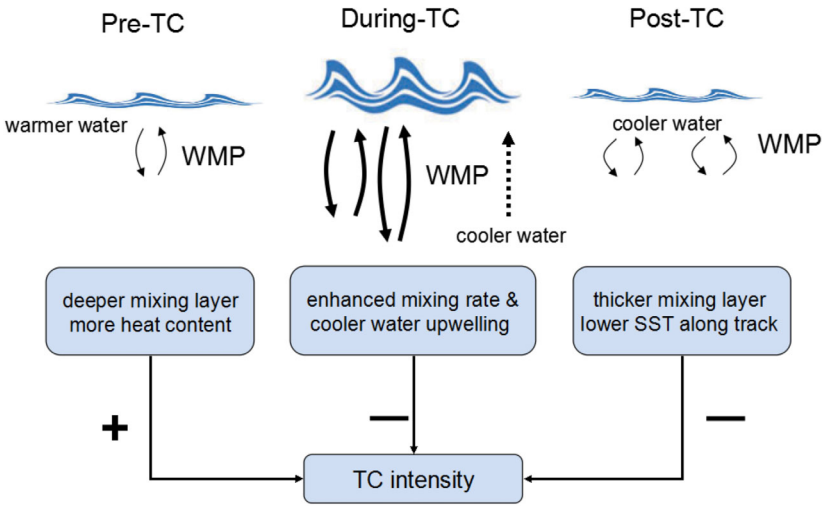

Figure 15. Schematic diagram illustrating the effect of including nonbreaking wave-stirring-induced mixing parameterization (WMP) to the ocean model on the upper ocean thermal structure and the TC intensity.

thicker and much closer to the observations in the upper 100 m. Therefore, the incorporation of WMP can improve the initial UOTS significantly. The deepened mixing layer at the initial time results in more initial heat content in the upper ocean, which helps to reduce the SST cooling in the TC simulation (i.e., a negative effect on the SST cooling). The incorporation of the WMP in the TC simulation (SIM_WMP/ALL_WMP), on the other hand, intensifies the SST cooling (i.e., a positive effect on the SST cooling) through the enhancement of upper ocean mixing rate, as indicated in Figure 14. Similar to the overestimated case Ketsana (2009), the SST cooling simulated by ALL_WMP is a compromise of the negative effect by including the WMP in the initialization and the positive effect by including the WMP in the TC simulation. The difference is that the two effects are comparable in ALL_WMP for the underestimated case (Figures 11a and 14), instead of the latter dominating over the former for the overestimated case (Figures 4a and 8). This is because the sea surface winds are seriously underestimated for the underestimated case (with a discrepancy of about 21.3 m s^{-1} for NON_WMP as shown in Table 2). Consequently, the enhancement of the ocean mixing rate by including the WMP in the TC simulation is not sufficient to bring up the cold water under the deepened thermocline formed by the initialization with the WMP included (Figure 14d). Therefore, for the underestimated TC case (the simulated winds are weak), it is the improved initial state of the UOTS by including the WMP in the initialization that prevents the typhoon from becoming much weaker.

5. Conclusions

In this study, the impacts of nonbreaking wave-stirring-induced mixing on the UOTS and TC intensity are investigated by incorporating a simple WMP scheme into a regional coupled atmosphere-ocean model for the South China Sea (SCS). The results of two selected typhoon cases indicate that including the WMP in the coupled model for the SCS has significant impact on the UOTS which in turn influences the TC intensity.

In particular, it is found that adding WMP to the ocean model can improve the SST simulation in the SCS in two ways (Figure 15): (1) improving the initial UOTS with a deepened MLD and (2) enhancing the total mixing rate in the TC simulation. The compromise of the negative effect on the SST cooling by including the WMP in the initialization and the positive effect by including the WMP in the TC simulation results in a better SST simulation in the coupled model no matter if the wind fields are overestimated or underestimated by the atmosphere model alone. When the simulated winds are weak (in the case that TC is underestimated by the atmosphere model alone), the effect of the improved initial UOTS from the initialization with the WMP is comparable to the mixing cooling effect and helps to prevent the TC from further weakening. When the simulated winds are strong (in the case that TC is overestimated by the atmosphere model), the enhancement of the vertical mixing rate by including the WMP dominates over the negative effect of the initial UOTS with the WMP on SST cooling and thus strengthens the SST cooling, resulting in a better TC intensity simulation with reduction of the averaged minimum SLP error compared to the tests without the

WMP. The results indicate that the nonbreaking wave-stirring-induced mixing is an important process during a TC passage in the SCS and including a WMP in a coupled model is recommended not only for the initialization but also for forecasting of a TC in the SCS.

It should be noted that, although the improvement of SST simulation/prediction could make a contribution to the ongoing efforts of improving the typhoon intensity forecast using a regional atmosphere-ocean coupled model, a better SST simulation by including a WMP in a coupled model does not guarantee a better TC intensity simulation due to the deficiency of physical parameterization or the insufficient resolution of the atmosphere models. In addition, a limit in the present study is that the wave parameters used in the wind-wave-induced mixing parameterization are obtained from the off-line run of a wave model. An atmosphere-ocean-wave full coupled model is expected to further improve the simulation of the nonbreaking wave-stirring-induced mixing process as well as the TC intensity in the SCS, which will be our future work.

Acknowledgments

This work was jointly supported by the Ministry of Science and Technology of the People's Republic of China (MOST) (2011CB403505, 2014CB953904), the Strategic Priority Research Program of the Chinese Academy of Sciences (XDA11010304), the Innovation Key Program of the Chinese Academy of Sciences (KZCX2-EW-208), the National Natural Science Foundation of China (41306013, 41376021, 41205032), the Youth Frontier Science Project of the South China Sea Institute of Oceanology (SQ200914), the Knowledge Innovation Program of the Chinese Academy of Sciences (SQ201305), and NOAA RUSALCA project to J.W. We thank Cathy Darnell of NOAA GLERL for editing this paper. This is GLERL contribution No. 1721. We gratefully acknowledge the use of the HPCC for all numeric simulations at the South China Sea Institute of Oceanology, Chinese Academy of Sciences and also thank Dr. John Bratton of NOAA GLERL for drafting Figure 15.

References

Ardhuin, F., and A. D. Jenkins (2006), On the interaction of surface waves and upper ocean turbulence, *J. Phys. Oceanogr.*, *36*, 551–557.

Babanin, A. V. (2006), On a wave-induced turbulence and a wave-mixed upper ocean layer, *Geophys. Res. Lett.*, *33*, L20605, doi:10.1029/2006GL027308.

Babanin, A. V., and B. K. Haus (2009), On the existence of water turbulence induced by nonbreaking surface waves, *J. Phys. Oceanogr.*, *39*, 2675–2679, doi:10.1175/2009JP04202.1.

Babanin, A. V., I. R. Young, and H. Mirfenderesk (2005), Field and laboratory measurements of wave–bottom interaction, in *Proceedings of the 17th Australasian Coastal and Ocean Engineering Conference and 10th Australasian Port and Harbour Conference*, edited by M. Townsend and D. Walker, pp. 293–298, Inst. of Eng., Canberra, Australia.

Babanin, A. V., A. Ganopolski, and W. R. C. Phillips (2009), Wave-induced upper-ocean mixing in a climate modelling of intermediate complexity, *Ocean Modell.*, *29*, 189–197.

Black, P. G., E. A. D'Asaro, T. B. Sanford, W. M. Drennan, J. A. Zhang, J. R. French, P. P. Niiler, E. J. Terrill, and E. J. Walsh (2007), Air–sea exchange in hurricanes: Synthesis of observations from the Coupled Boundary Layer Air–Sea Transfer experiment, *Bull. Am. Meteorol. Soc.*, *88*, 357–374.

Blumberg, A. F., and G. L. Mellor (1987), A description of a three-dimensional coastal ocean circulation model, in *Three-Dimensional Coastal Ocean Models*, edited by N. S. Heaps, pp. 1–16, AGU, Washington, D. C.

Boyer, T. P., C. Stephens, J. I. Antonov, M. E. Conkright, R. A. Locarnini, T. D. O'Brien, and H. E. Garcia (2002), *World Ocean Atlas 2001,* vol. 1, *Salinity*, NOAA Atlas NESDIS 50, edited by S. Levitus, pp. 176–182, U.S. Gov. Print. Off., Washington, D. C.

Cai, S. Q., and Z. J. Gan (2000), The application of a three-dimensional baroclinic shelf sea model: The seasonal variation of the South China Sea upper mixed layer [in Chinese], *Acta Oceanol. Sin.*, *22*(3), 7–14.

Carton, J. A., G. Chepurin, X. Cao, and B. Giese (2000a), A simple ocean data assimilation analysis of the global upper ocean 1950–1995. Part I: Methodology, *J. Phys. Oceanogr.*, *30*, 294–309.

Carton, J. A., G. Chepurin, and X. Cao (2000b), A simple ocean data assimilation analysis of the global upper ocean 1950–1995. Part II: Results, *J. Phys. Oceanogr.*, *30*, 311–326.

Dai, D., F. Qiao, W. Sulisz, L. Han, and A. Babanin (2010), An experiment on the nonbreaking surface-wave-induced vertical mixing, *J. Phys. Oceanogr.*, *40*(9), 2180–2188.

Donelan, M. A., B. K. Haus, N. Reul, W. J. Plant, M. Stiassnie, H. C. Graber, O. B. Brown, and E. S. Saltzman (2004), On the limiting aerodynamic roughness of the ocean in very strong winds, *Geophys. Res. Lett.*, *31*, L18306, doi:10.1029/2004GL019460.

Dudhia, J. (1989), Numerical study of convection observed during the Winter Monsoon Experiment using a mesoscale twodimensional model, *J. Atmos. Sci.*, *46*, 3077–3107.

Emanuel, K. A. (2003), A similarity hypothesis for air–sea exchange at extreme wind speeds, *J. Atmos. Sci.*, *60*, 1420–1428.

Emanuel, K., C. DesAutels, C. Holloway, and R. Korty (2004), Environmental control of tropical cyclone intensity, *J. Atmos. Sci.*, *61*, 843–858.

Evans, A., and B. Falvey (2013), An overview of joint typhoon warning center tropical cyclone forecast improvement focus, paper presented at 67th Interdepartmental Hurricane Conference, NOAA Center for Weather and Climate Prediction College Park, Md. [Available at http://www.ofcm.gov/ihc13/Presentations/4-Session/05-S4-JTWC_IHC-2013.pptx.]

Ferrier, B. S., Y. Lin, T. Black, E. Rogers, and G. Di Mego (2002), Implementation of a new grid-scale cloud and precipitation scheme in the NCEP Eta model, in *15th Conference on Numerical Weather Prediction*, pp. 280–283, Am. Meteorol. Soc., San Antonio, Tex.

Gayer, G., S. Dick, A. Pleskachevsky, and W. Rosenthal (2006), Numerical modeling of suspended matter transport in the North Sea, *Ocean Dyn.*, *56*, 62–77.

Ginis, I. (2002), Tropical cyclone–ocean interactions, in *Atmosphere-Ocean Interactions, Adv. Fluid. Mech.*, No. 33, edited by W. Perrie, pp. 83–114, WIT Press, Bedford Institute of Oceanography, Canada.

Hendricks, E. A., M. S. Peng, B. Fu, and T. Li (2010), Quantifying environmental control on tropical cyclone intensity change, *Mon. Weather Rev.*, *138*(8), 3243–3271.

Hong, S. Y., Y. Noh, and J. Dudhia (2006), A new vertical diffusion package with an explicit treatment of entrainment processes, *Mon. Weather Rev.*, *134*, 2318–2341.

Hu, H., and J. Wang (2010), Modeling effects of tidal and wave mixing on circulation and thermohaline structures in the Bering Sea: Process studies, *J. Geophys. Res.*, *115*, C01006, doi:10.1029/2008JC005175.

Hu, H., Y. Yuan, and Z. Wan (2004), Study on hydrodynamics of the Bohai Sea, the Yellow Sea and the East China Sea with wave-current coupled numerical model [in Chinese with English abstract], *Acta Oceanol. Sin.*, *4*, 19–32.

Huang, C., and F. Qiao (2010), Wave–turbulence interaction and its induced mixing in the upper ocean, *J. Geophys. Res.*, *115*, C04026, doi:10.1029/2009JC005853.

Huang, C. J., F. Qiao, Q. Shu, and Z. Song (2012), Evaluating austral summer mixed-layer response to surface wave-induced mixing in the Southern Ocean, *J. Geophys. Res.*, *117*, C00J18, doi:10.1029/2012JC007892.

Kain, J. S., and J. M. Fritsch (1990), A one-dimensional entraining/detraining plume model and its application in convective parameterization, *J. Atmos. Sci.*, *47*, 2784–2802.
Kain, J. S., and J. M. Fritsch (1993), Convective parameterization for mesoscale models: The Kain-Fritsch scheme, in *The Representation of Cumulus Convection in Numerical Models, Meteor. Monogr.*, No. 24, edited by K. A. Emanuel and D. J. Raymond, pp. 165–170, Am. Meteorol. Soc., Boston, Mass.
Kalnay, E., et al. (1996), The NCEP/NCAR 40-year reanalysis project, *Bull. Am. Meteorol. Soc.*, *77*(3), 437–471, doi:10.1175/1520-0477(1996)077.
Kim, H.-S., C. Lozano, V. Tallapragada, D. Iredell, D. Sheinin, H. L. Tolman, V. M. Gerald, and J. Sims (2014), Performance of ocean simulations in the coupled HWRF–HYCOM model, *J. Atmos. Oceanic Technol.*, *31*, 545–559.
Large, W. G., and S. G. Yeager (2009), The global climatology of an interannually varying air-sea flux data set, *Clim. Dyn.*, *33*, 341–364, doi: 10.1007/s00382-008-0441-3.
Marks, F. D., and L. K. Shay (1998), Landfalling tropical cyclones: Forecast problems and associated research opportunities, *Bull. Am. Meteorol. Soc.*, *79*, 305–323.
Marks, K. M., and W. H. F. Smith (2006), An evaluation of publicity available global bathymetry grids, *Mar. Geophys. Res.*, *27*, 19–34.
Martin, P. J. (1985), Simulation of the mixed layer at OWS November and Papa with several models, *J. Geophys. Res.*, *90*, 903–916, doi: 10.1029/JC090iC01p00903.
Mellor, G. L. (2004), *Users Guide for a Three-Dimensional, Primitive Equation, Numerical Ocean Model* (June 2003 version), 53 pp., Prog. in Atmos. and Ocean. Sci., Princeton Univ. Press, Princeton, N. J.
Mellor, G. L., and A. F. Blumberg (2004), Wave breaking and ocean surface layer thermal response, *J. Phys. Oceanogr.*, *34*, 693–698.
Mellor, G. L., and T. Yamada (1982), Development of a turbulence closure model for geophysical fluid problems, *Rev. Geophys. Space Phys.*, *20*, 851–875.
Mlawer, E. J., S. J. Taubman, P. D. Brown, M. J. Iacono, and S. A. Clough (1997), Radiative transfer for inhomogeneous atmosphere: RRTM, a validated correlated-k model for the longwave, *J. Geophys. Res.*, *102*, 16,663–16,682.
Ooyama, K. (1969), Numerical simulation of the life-cycle of tropical cyclones, *J. Atmos. Sci.*, *26*, 3–40.
Pleskachevsky, A., M. Dobrynin, A. V. Babanin, H. Günther, and E. Stanev (2011), Turbulent mixing due to surface waves indicated by remote sensing of suspended particulate matter and its implementation into coupled modeling of waves, turbulence, and circulation, *J. Phys. Oceanogr.*, *41*, 708–724.
Powell, M. D., P. J. Vickery, and T. A. Reinhold (2003), Reduced drag coefficient for high wind speeds in tropical cyclones, *Nature*, *422*, 279–283.
Qiao, F., Y. Yuan, Y. Yang, Q. Zheng, C. Xia, and J. Ma (2004), Wave induced mixing in the upper ocean: Distribution and application to a global ocean circulation model, *Geophys. Res. Lett.*, *31*, L11303, doi:10.1029/2004GL019824.
Qiao, F., Y. Yang, C. Xia, and Y. Yuan (2008), The role of surface waves in the ocean mixed layer, *Acta Oceanol. Sin.*, *27*(3), 30–37.
Qiao, F., Y. Yuan, T. Ezer, C. Xia, Y. Yang, X. Lü, and Z. Song (2010), A three-dimensional surface wave-ocean circulation coupled model and its initial testing, *Ocean Dyn.*, *60*(5), 1339–1355, doi:10.1007/s10236-010-0326-y.
Shay, L. K., G. J. Goni, and P. G. Black (2000), Effects of a warm oceanic feature on Hurricane Opal, *Mon. Weather Rev.*, *128*, 1366–1383.
Skamarock, W. C., J. B. Klemp, J. Dudhia, D. O. Gill, D. M. Barker, W. Wang, and J. G. Powers (2007), A description of the advanced research WRF version 2, *Tech. Note NCAR/TN-4681STR*, 88 pp., Natl. Cent. for Atmos. Res., Boulder, Colo.
Su, J. L. (2004), Overview of the South China Sea circulation and its influence on the coastal physical oceanography outside the Pearl River Estuary, *Cont. Shelf Res.*, *24*, 1745–1760.
Terray, E. A., M. A. Donelan, Y. C. Agrawal, W. M. Drennan, K. K. Kahma, A. J.Williams III, P. A. Hwang, and S. A. Kitaigorodskii (1996), Estimates of kinetic energy dissipation under breaking waves, *J. Phys. Oceanogr.*, *26*, 792–807.
Toffoli, A., J. McConochie, M. Ghantous, L. Loffredo, and A. V. Babanin (2012), The effect of wave-induced turbulence on the ocean mixed layer during tropical cyclones: Field observations on the Australian North-West Shelf, *J. Geophys. Res.*, *117*, C00J24, doi:10.1029/2011JC007780.
Tolman, H. L. (2009), User manual and system documentation of WAVEWATCH III version 3.14, *Tech. Note 276*, 194 pp., Natl. Oceanic Atmos. Admin., Camp Springs, Md.
Valcke, S., L. Terray, and A. Piacentini (2000), The OASIS Coupler User's Guide, Version 2.4, *Tech. Rep. TR/CGMC/00–10*, 85 pp., CERFACS, Toulouse, France.
Wang, J. (1996), Global linear stability of the 2-D shallow water equations: An application of the distributive theorem of roots for polynomials on the unit circle, *Mon. Weather Rev.*, *124*(6), 1301–1310.
Wang, W., D. Barker, J. Bray, C. Bruyère, M. Duda, J. Dudhia, D. Gill, and J. Michalakes (2007), *WRF Version 2 Modeling System User's Guide*, NCAR MMM Tech. Note. USA. [Available at http://www.mmm.ucar.edu/wrf/users/docs/user_guide/.]
Wu, B., and J. Wang (2002a), Winter Arctic Oscillation, Siberian High and the East Asia winter monsoon, *Geophys. Res. Lett.*, *29*(19), 1897, doi:10.1029/2002GL015373.
Wu, B., and J. Wang (2002b), Possible impacts of winter Arctic Oscillation on Siberian High and the East Asia winter monsoon, *Adv. Atmos. Sci.*, *19*, 297–320.
Wu, C. C., and Y. H. Kuo (1999), Typhoons affecting Taiwan: Current understanding and future challenges, *Am. Meteorol. Soc.*, *80*(1), 67–80.
Wyrtki, K. (1961), Physical oceanography of the Southeast Asia waters, *NAGA Rep. 2*, pp. 1–195, The University of California Scripps Institution of Oceanography, La Jolla, Calif.
Zhang, Y. C., and Y. F. Qian (1999), Numerical simulation of the regional ocean circulation in the coastal area of China, *Adv. Atmos. Sci.*, *16*(3), 443–450.